Journal of Alloys and Compounds 512 (2012) 17–22

Contents lists available at ScienceDirect

Journal of Alloys and Compounds

journal homepage: www.elsevier.com/locate/jallcom

Effect of structural distortion and nature of bonding on the electronic properties of defect and Li-substituted $CuInSe_2$ chalcopyrite semiconductors

S. Mishra, B. Ganguli *

National Institute of Technology, Rourkela 769008, Odisha, India

ARTICLE INFO

Article history:
Received 30 March 2011
Received in revised form 6 August 2011
Accepted 8 August 2011
Available online 31 August 2011

Keywords:
Chalcopyrite
Semiconductors
Density functional theory
TB-LMTO

ABSTRACT

We report the structural and electronic properties of chalcopyrite semiconductors $CuInSe_2$, $CuIn_2Se_4$ and $Cu_{0.5}Li_{0.5}InSe_2$. Our calculation is based on density functional theory within tight binding linear muffin-tin orbital (TB-LMTO) method. The calculated lattice constants, anion displacement parameter (u), tetragonal distortion parameter ($\eta = c/2a$) and bond lengths agree well with experimental values. Our result shows these compounds are direct band gap semiconductors. Our calculated band gaps, 0.79 eV and 1.08 eV of $CuInSe_2$ and $Cu_{0.5}Li_{0.5}InSe_2$, respectively, agree well with the experimental values within the limitation of LDA. The band gap of $CuIn_2Se_4$ is found to be 1.50 eV. The band gap is reduced by 59.57%, 23.61% and 48.82% due to p–d hybridization and reduced by 16.85%, 9.10% and 0.92% due to structural distortion for $CuInSe_2$, $CuIn_2Se_4$ and $Cu_{0.5}Li_{0.5}InSe_2$, respectively. We also discuss the effect of bond nature on electronic properties of all three compounds.

1. Introduction

Among the $A^{I}–B^{III}–C_2^{VI}$ compounds, $CuInSe_2$, having band gap energy 1.04 eV [1], is regarded as one of the best investigated materials for thin film solar cells. But partial Li-substitution in place of Cu atoms not only changes its physical properties but also tailors the energy band gap to be suitable for optimum conversion efficiency for solar cells. The defect is that chalcopyrites have vacancies at the cation sites in an ordered manner to maintain the periodicity of the crystal. This means these are ordered vacancy compounds (OVC) [2]. Due to the defect structure the compounds are porous. Because of porousity these systems have attracted special attention in the physics community. Various type of impurities including magnetic impurities can be doped/substituted into the vacancies to design a new class of materials, like dilute magnetic semiconductors (DMS) for spintronics application [3], optoelectronic devices [4] and solar cells [5]. The presence of vacancies, and more than two type of atoms provide desired band gap, electronic and optical properties for new emerging functional materials.

In this communication we investigate a comparative study of the structural, electronic properties and bond nature of $CuInSe_2$, $CuIn_2Se_4$ and $Cu_{0.5}Li_{0.5}InSe_2$ compounds. There are very few experimental [6] and theoretical [7] studies carried out for $CuIn_2Se_4$. Suzuki et al. [7] carried out band structure calculation of chalcopyrite $CuInSe_2$, stannite $CuIn_3Se_5$ and defect stannite $CuIn_2Se_4$. No theoretical study for $Cu_{0.5}Li_{0.5}InSe_2$ has been reported till date. Mitaray et al. [8] studied the growth, structure and optical properties of $Cu_{1-x}Li_xInSe_2$ thin films. They found that $Cu_{0.5}Li_{0.5}InSe_2$ has the chalcopyrite structure and is a direct band gap semiconductor for $x \leq 0.6$. Weise et al. [9] discussed the preparation and the structural phase transformation of $Cu_{1-x}Li_xInSe_2$. They also reported this to have the chalcopyrite structure below 810 °C for $0 \leq x \leq 0.55$. Extensive experimetal [10–13] and theoretical studies [14,15] have been carried out for $CuInSe_2$. This compound is found to have chalcopyrite structure having space group $I\bar{4}2d$ [15]. We choose this already much studied system to validate our methodology and calculation and extend the study to two other systems which have not been much studied. Our main motivation is to study the effect of structural distortion and p–d hybridization on the electronic properties. We consider here two types of structural distortions, the displacement of anions from their ideal position (included in the parameter 'u') and structural deformation expressed by the ratio of the lattice parameters ($c/2a$). We also discuss the bond nature of these compounds. In our earlier work on pure chalcopyrite semiconductors [16] and defect chalcopyrite systems [17], we show that due to the presence of group I element (Cu,Ag), d-orbital contribution is very prominent. The main contribution of d-orbitals to upper valence band is significant which affects band gap. In case of $Cu_{0.5}Li_{0.5}InSe_2$, though lithium has no d-orbital contribution, its substitution has significant effect on Cu d and Se p hybridization. For structural properties, we calculate the lattice parameters, tetragonal distortion, anion displacement parameters and bond lengths by energy minimization proceedure. We also calculate the bulk modulus for $CuIn_2Se_4$ using extended Cohens formula [18] and we

---

* Corresponding author. Tel.: +91 661 2462725; fax: +91 661 24629990.
E-mail address: biplabg@nitrkl.ac.in (B. Ganguli).

0925-8388/$ – see front matter © 2011 Elsevier B.V. All rights reserved.
doi:10.1016/j.jallcom.2011.08.040

extend this formula to calculate bulk modulus for $Cu_{0.5}Li_{0.5}InSe_2$. There have been no calculation so far of bulk modulus of these two compounds. For our study we use highly successful density functional theory (DFT) based first principle technique, tight binding linearized muffin-tin orbital (TB-LMTO) method. In TB-LMTO method, the basis functions are localized. Therefore, very few basis functions are required to represent the highly localized d-orbital of Cu in the systems under study. Hence the calculation is not only cost effective, it gives also accurate results.

2. Methodology

The ab initio method is based on density functional theory of Kohn–Sham [19]. The one electron energy is given by Kohn–Sham equation:

$$[-\nabla^2 + V_{\text{eff}}(r)]\psi_i(r) = \varepsilon_i \psi_i(r) \tag{1}$$

where the effective potential:

$$V_{\text{eff}}(r) = 2\int \frac{\rho(r')}{|r-r'|}\,dr' - 2\sum_R \frac{Z_R}{|r-R|} + \frac{\delta E_{XC}[\rho]}{\delta\rho(r)} \tag{2}$$

The total electronic energy is a function of electron density which is calculated using variational principle. This requires self consistent calculations. In practice the Kohn–Sham orbitals $\psi_i(r)$ are usually expanded in terms of some chosen basis function. We use the well established TB-LMTO method, discussed in detail elsewhere [20,21] for the choice of the basis function. Electron correlations are taken within LDA of DFT [19,22]. We use the von Barth–Hedin exchange [23] with 512 k-points in the irreducible part of the Brillouin zone. The basis of the TB-LMTO starts from the minimal set of muffin-tin orbitals of a KKR formalism and then linearizes it by expanding around a 'nodal' energy point $E^{\alpha}_{\nu\ell}$. The wave-function is then expanded in this basis:

$$\Phi_{jk}(r) = \sum_L \sum_\alpha c^{jk}_{L\alpha}\left[\phi^{\alpha}_{\nu L}(r) + \sum_{L'}\sum_{\alpha'} h^{\alpha\alpha'}_{LL'}(k)\,\dot{\phi}^{\alpha'}_{\nu L'}(r)\right] \tag{3}$$

where

$$\phi^{\alpha}_{\nu L}(r) = i^{\ell} Y_L(\hat{r})\phi^{\alpha}_{\ell}(r, E^{\alpha}_{\nu\ell})$$

$$\dot{\phi}^{\alpha}_{\nu L}(r) = i^{\ell} Y_L(\hat{r})\frac{\partial\phi^{\alpha}_{\ell}(r, E^{\alpha}_{\nu\ell})}{\partial E}$$

$$h^{\alpha\alpha'}_{LL'}(k) = (C^{\alpha}_L - E^{\alpha}_{\nu\ell})\delta_{LL'}\delta_{\alpha\alpha'} + \sqrt{\Delta^{\alpha}_L}S^{\alpha\alpha'}_{LL'}(k)\sqrt{\Delta^{\alpha'}_{L'}}$$

C^{α}_L and Δ^{α}_L are TB-LMTO potential parameters and $S^{\alpha\alpha'}_{LL'}(k)$ is the structure matrix.

3. Result and discussion

3.1. Structural properties

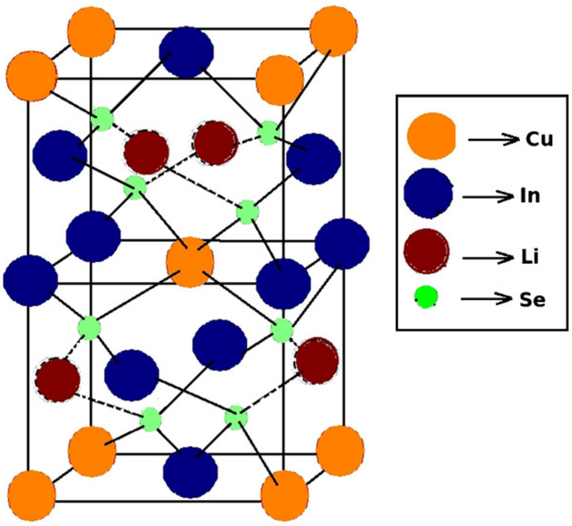

Fig. 1. One unit cell of $Cu_{0.5}Li_{0.5}InSe_2$.

A typical chalcopyrite unit cell contains two types of cations resulting in a unit cell twice as large as that of zinc blende and a reduction in symmetry to the tetragonal system. In a defect chalcopyrite there is a 50% vacancy in one type of cation compared to pure chalcopyrite. Thus such defect compounds fall under vacancy defect systems. Similar definition of defect system has been also used by other authors [2,7]. In Li-substituted $CuInSe_2$ there are three types of cations in a unit cell unlike pure and defect chalcopyrites. One unit cell of $Cu_{0.5}Li_{0.5}InSe_2$ is shown in Fig. 1. In $Cu_{0.5}Li_{0.5}InSe_2$, 50% of the Cu atoms is substituted by Li-atoms. In both defect and Li-substituted $CuInSe_2$, the vacancies/Li atoms are occupied in such a manner that they maintain periodicity. Thus the system is an ordered-defect compound [2]. There are two Cu atoms, two Li atoms, four In atoms and eight Se atoms per unit cell. The positions of the various atoms in the tetragonal unit cell of $CuInSe_2$ are: Cu on 4a site (0,0,0) & (0,0.5,0.25), In on 4b site (0,0,0.5) & (0,0.5,0.75), Se on 8d site (u,0.25,0.125) where 'u' is anion displacement parameter. The structure of $CuInSe_2$ is chalcopyrite having space group $I\bar{4}2d$. In the defect and Li-substituted $CuInSe_2$ the positions of the various atoms in the tetragonal unit cell are: Cu on 2a site (0,0,0), In1 on 2b site (0,0,0.5), In2 on 2d site (0,0.5,0.75), vacancy/Li on 2c site (0,0.5,0.25) and Se on 8g site (u_x,u_y,u_z) where 'u_x', 'u_y' and 'u_z' are anion displacement parameters along three axes. The space group of the defect chalcopyrite $CuIn_2Se_4$ and $Cu_{0.5}Li_{0.5}InSe_2$ is $I\bar{4}$ (S_4^2). Suzuki et al. [7] studied the same defect compound $CuIn_2Se_4$ but they considered it as defect stannite structure. In their case the position of various atoms are Cu on '2a' site, In on '2c' and '2d' sites, vacancy on '2b' site and Se on '8i' site. Therefore, they created vacancy on In site ('2b' site) in the stannite compound $CuIn_3Se_5$. So they called $CuIn_2Se_4$, a defect stannite compound. Unit cell with $\eta = 1$, u_x, u_y and u_z equal to 0.25, 0.25 and 0.125, respectively, is refered as ideal case. This is defined in analogous to binary zinc-blende (ZnS) structure [15]. In $CuIn_2Se_4$ system, each Se atom has one Cu cation, two In cations and one vacancy as nearest neighbors. Due to different atoms and one vacancy as neighbors, Se atom acquires an equlibrium position closer to the vacancy than to the other three cations. Whereas, in case of $Cu_{0.5}Li_{0.5}InSe_2$, as shown in Fig. 1, each Se atom has one Cu cation, two In cations and one Li atom as nearest neighbors. The Se atom moves towards the Li atom to acquire the equilibrium position. This new position of anion is called anion displacement. In both defect and Li-substituted $CuInSe_2$, Se atoms shift along all the three directions unlike only along x-direction as found in the case of $CuInSe_2$ chalcopyrites [15]. This is due to the reduction in symmetry in case of $CuIn_2Se_4$ and $Cu_{0.5}Li_{0.5}InSe_2$ systems. Therefore, all cations–Se bond lengths are inequivalent in

Table 1
Calculated structural parameters.

Compounds	a (Å)	$c/2a$	a_{exp} (Å)	$c/2a_{\text{exp}}$	u_x(exp)	u_x	u_y	u_z	B (GPa)	Space group
$CuInSe_2$	5.75	1.010	5.78[a]	1.005[a]	0.235[a]	0.236	0.250	0.125		$I\bar{4}2d$
$CuIn_2Se_4$	5.74	1.014				0.251	0.235	0.126	45.44	$I\bar{4}$
$Cu_{0.5}Li_{0.5}InSe_2$	5.84	0.996	5.85[b]	0.994[b]		0.253	0.233	0.127	60.14	$I\bar{4}$

[a] Ref. [24].
[b] Ref. [9].

Table 2
Calculated bond lengths in Å.

Systems	R_{Cu-Se} (Å)	R_{In1-Se} (Å)	R_{In2-Se} (Å)	$R_{(Cu/\text{Vacancy}/Li)-Se}$ (Å)
$CuInSe_2$	2.452	2.543	2.543	2.452
$CuIn_2Se_4$	2.458	2.551	2.544	2.438
$Cu_{0.5}Li_{0.5}InSe_2$	2.492	2.587	2.574	2.445

defect and Li-substituted $CuInSe_2$ whereas, this is not the case for $CuInSe_2$ [15] (Table 1). Calculated bond lengths are listed in Table 2. For self consistent calculation, we introduce empty spheres because the packing fraction is low due to tetrahedral coordination of ions. We ensure proper overlap of muffin tin spheres for self consistency and the percentage of overlap is found. Table 1 shows the calculated lattice parameters 'a' & 'c', tetragonal distortion, anion displacement and bulk modulus (B). These parameters are found by energy minimization proceedure. We calculate the bulk modulus 'B' for $CuIn_2Se_4$ using extended Cohen formula [18]. The bulk modulus of $Cu_{0.5}Li_{0.5}InSe_2$ is calculated by the slightly modified form of extended Cohen formula given in Eq. (4):

$$B = \frac{1971 - 220\lambda}{4} \sum_{i=1,2,3,4} \frac{1}{d_i^{3.5}} \tag{4}$$

where B is in GPa and the nearest-neighbor distances d_i in A^0. The distances d_i in Eq. (4) are the bond lengths of Cu–Se, Li–Se, In1–Se and In2–Se. The ionicity coefficient λ is taken equal to 2, analogous to II–VI semiconductors [18].

3.2. *Electronic properties*

3.2.1. $CuInSe_2$

Our result shows this compound a direct band gap semiconductor. Total density of states (TDOS) (Fig. 2(a)) shows four major sub valence bands of different band widths. The first two subbands below the valence band maximum have band widths 1.9 eV and 2.7 eV, respectively. They are separated by very narrow band gap of 0.95 eV. The third and fourth subbands have band width 0.8 eV and 1.3 eV, respectively. They are separated by a large band gap of 6.4 eV. The second and third subbands are separated by a very narrow band gap of 0.3 eV. The major contribution for the formation of the first subband comes from Cu d orbitals and weak contribution from Se p orbitals. Whereas, it is other way round for the formation of the second subband. Contribution for the formation of the third subband comes from the admixture of In s and Se p orbitals. The lowest subband is Se 4s band. Fig. 2(b) shows partial density of states (PDOS) for Cu-d and Se-p. It is clear from the figure that Cu d and Se p hybridization contribute to upper valence band near Fermi level and there is no contribution of Cu d states to conduction band. The main contribution to the conduction band comes from Cu p, In p and Se p states and very weak contribution from Cu s and In s orbitals. The conduction band width is 16.0 eV. Our band structure result agrees with the work of Jaffe and Zunger [15].

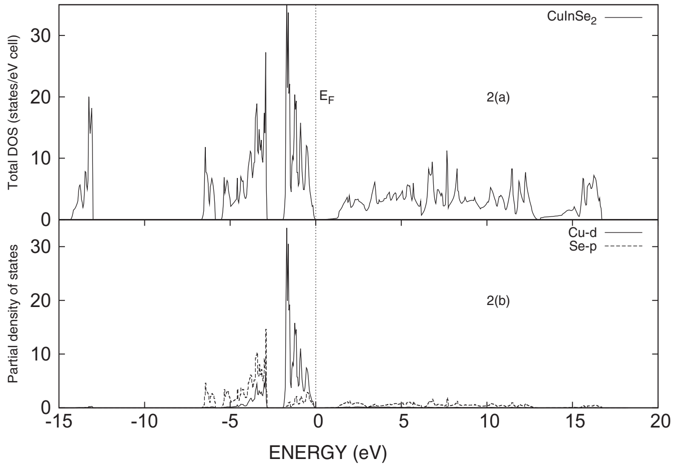

Fig. 2. (a) TDOS of $CuInSe_2$ and (b) PDOS of Cu d and Se p orbitals of $CuInSe_2$.

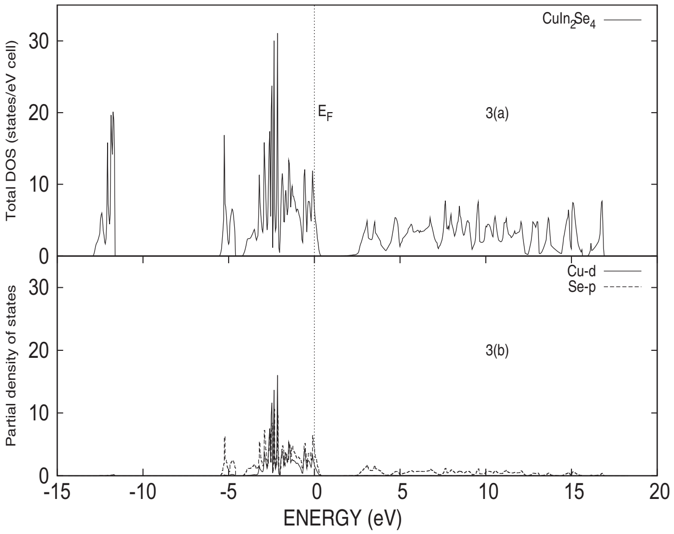

Fig. 3. (a) TDOS of $CuIn_2Se_4$ and (b) PDOS of Cu d and Se p orbitals of $CuIn_2Se_4$.

3.2.2. $CuIn_2Se_4$

Unlike $CuInSe_2$, this compound is slightly p-type semiconductor. TDOS (Fig. 3(a)), shows three sub valence bands of different band widths. The first two subbands have band widths 4.6 eV and 1.0 eV, respectively, and are separated by very narrow band gap of 0.4 eV. The lowest subband with band width 1.3 eV is Se 4s band. There is a large band gap of nearly 6.1 eV between the lowest and second subband. Contribution for the second subband comes from the admixture of In s and Se p states. Calculated PDOS (Fig. 3(b)) shows that the upper valence band is dominated by Cu d and Se p hybride orbitals. This semiconductor shows p-type conductivity because Se p orbitals cross Fermi level. The conduction band width is approximately 14.9 eV. The main contribution comes from Cu p, In p and Se p states and a very weak contribution from Cu s and In s states for the formation of the conduction band.

3.2.3. *(iii)* $Cu_{0.5}Li_{0.5}InSe_2$

The band structure and TDOS (Fig. 4) show four major sub valence bands of different band widths. The two upper most subvalence bands have band widths of 1.2 eV and 3.1 eV, respectively. They are separated by 0.4 eV. Calculated PDOS (Fig. 5(b)) of Cu d and Se p orbitals show that the main contribution to the upper most sub valence band comes from Cu d orbital and very weak contribution comes from Se p orbitals. The second sub valence band is mainly formed due to the contribution of Se p and very weak contribution from Cu d states like in the case of $CuInSe_2$. The lowest band of band width 1.2 eV is formed due to the contribution of Se 4s states. The third sub valence band is formed due to the admixture of In s and Se p orbitals. The main contribution to conduction band comes from Cu p, Se p, In p and very weak contribution comes from In s and Li s orbitals. From PDOS of Li s and Li p orbitals (Fig. 5(a)), we do not find any significant participation of Li-orbitals neither in valence band nor in conduction band. The conduction band width is found to be 15.2 eV.

In all the cases, valence band maximum (VBM) and conduction band minimum (CBM) are located at the center of Brillouin zone denoted as 'G' (Γ point). This indicates that they are all direct band

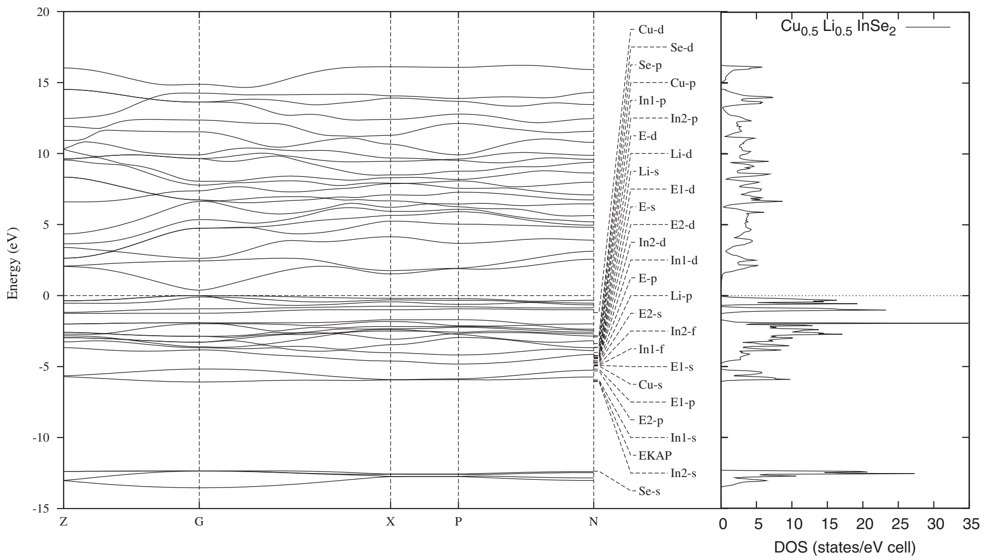

Fig. 4. Band structure and TDOS for non-ideal $Cu_{0.5}Li_{0.5}InSe_2$.

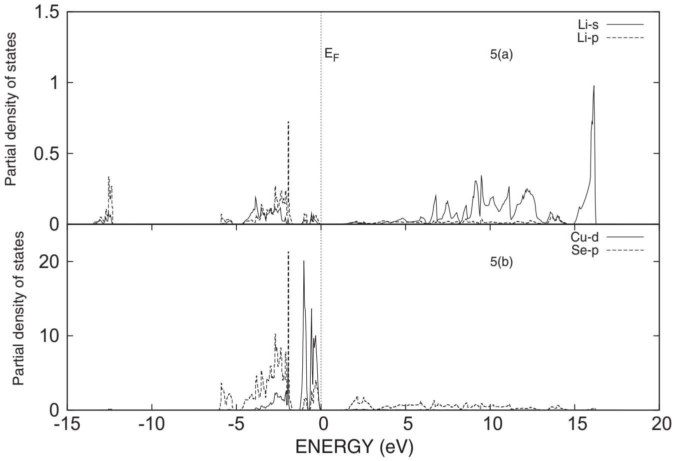

Fig. 5. (a) PDOS of Li s and Li p; (b) PDOS of Cu d and Se p orbitals in $Cu_{0.5}Li_{0.5}InSe_2$.

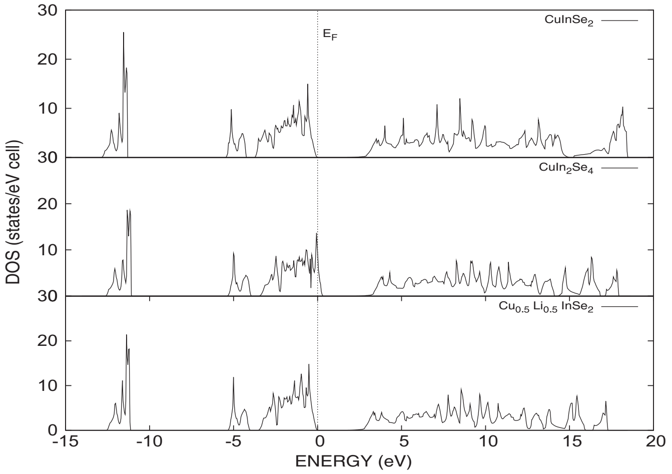

Fig. 6. TDOS of ideal (a) $CuInSe_2$, (b) $CuIn_2Se_4$ and (c) $Cu_{0.5}Li_{0.5}InSe_2$ without hybridization.

gap compounds. Experimental and our calculated band gaps are listed in Table 3. It is known that LDA underestimates band gap by 30–50% [25]. Within this LDA limitation, our results are in good agreement with experimental band gap. Suzuki et al. [7] have calculated band gap of defect stannite $CuIn_2Se_4$ to be 0.5 eV which is much below the experimental value 1.04–1.27 eV [6]. No detailed theoretical study of band gap for $Cu_{0.5}Li_{0.5}InSe_2$ is reported in literature.

3.3. Effect of p–d hybridization on electronic properties

It is known that p–d hybridization has significant effect on the band gap in the case of Cu based compounds like $CuInSe_2$ [15]. To see this effect explicitely, we calculate the TDOS without the contribution of the d-orbitals for ideal $CuInSe_2$, $CuIn_2Se_4$ and $Cu_{0.5}Li_{0.5}InSe_2$ systems. Therefore, we first freeze d-electrons and treat these electrons as core electrons. Fig. 6 shows the TDOS with d-electron of A atoms as frozen for all three systems, respectively. We summarize the band gaps with and without contribution of d-electrons of Cu in Table 4. The calculated result shows that there is a significant reduction of band gaps in all the cases. The reduction is 59.57% for $CuInSe_2$, 23.61% for $CuIn_2Se_4$ and 48.82% for $Cu_{0.5}Li_{0.5}InSe_2$. The p–d hybridization in chalcopyrite semiconductors can be interpreted on the basis of simple molecular orbital considerations [15]. The p-orbitals that possess the Γ_{15} symmetry hybridize with those of the d-orbitals that present the same symmetry. This hybridization forms a lower bonding state and an upper antibonding state. The

Table 3
Energy band gaps of chalcopyrites.

Compounds	Experiment (eV)	Our work (eV)
$CuInSe_2$	1.04[a]	0.79
$CuIn_2Se_4$	1.04–1.27[b]	1.50
$Cu_{0.5}Li_{0.5}InSe_2$	1.5[c]	1.08

[a] Ref. [1].
[b] Ref. [6].
[c] Ref. [9].

Table 4
% of reduction in band gap (eV) due to p–d hybridization for ideal case.

Systems	With hybridization	Without hybridization	Reduction (%)
$CuInSe_2$	0.95	2.35	59.57
$CuIn_2Se_4$	1.65	2.16	23.61
$Cu_{0.5}Li_{0.5}Se_2$	1.09	2.13	48.82

Table 5
Effect of structural distortion on band gap (eV).

Systems	Ideal	Non-ideal	% of decrement in band gap
$CuInSe_2$	0.95	0.79	16.85
$CuIn_2Se_4$	1.65	1.5	9.10
$Cu_{0.5}Li_{0.5}InSe_2$	1.09	1.08	0.92

antibonding state that constitutes the top of the valence band is predominantly formed by higher energy anion p-states and the bonding state is constituted by the lower energy cation d-states. Perturbation theory [26] suggests that the two states Γ_{15}(p) and Γ_{15}(d) will repel each other by an amount inversely proportional to the energy difference between p and d states. So this raising of the upper most state causes a gap reduction. But in defect $CuIn_2Se_4$ and Li substituted chalcopyrites, there is a reduction in the atomic percentage of Cu relative to that $CuInSe_2$. This reduces the symmetry. So the repulsion between Γ_{15}(p) and Γ_{15}(d) decreases and the antibonding state is depressed downwards leading to an increase in band gap. Therefore, all the Cu defficient defect chalcopyrites have band gaps greater than that the corresponding pure chalcopyrites. Since Li d-orbitals do not contribute to the valence band, we expect the reduction in band gap due to p–d hybridization in $Cu_{0.5}Li_{0.5}InSe_2$ and $CuIn_2Se_4$ to be equal, as both have equal concentration of Cu. Contrary to this, our calculation shows band gap reduction due to p–d hybridization in the Li-substituted $CuInSe_2$, is much more than the defect $CuIn_2Se_4$. On comparing TDOS for $CuIn_2Se_4$ (Fig. 3(a)) and $Cu_{0.5}Li_{0.5}InSe_2$ (Fig. 4), we find the conduction band minimum in the case of Li-substituted compound shifts significantly towards the Fermi level compared to the defect system. This shift is due to the shift of Se-p orbitals towards the Fermi level (Fig. 5(b)) in $Cu_{0.5}Li_{0.5}InSe_2$. The valence band maximum which lies slightly above the Fermi level in $CuIn_2Se_4$, shifts at the Fermi level in Li-substituted compound. There is very negligible contribution of Li-orbitals to valence and conduction bands. Therefore, we can say Li acts as a catalyst.

3.4. Structural effect on electronic properties

Table 5 shows the structural distortion like bond alternation and tetragonal distortion have some effect on the band gap. A close comparision of TDOS for ideal (Fig. 7) and non-ideal case (Figs. 2(a), 3(a) and 4) of all three compounds show distinct differences in the structure in DOS. For example a sharp peak is found at an energy −2.0 eV for nonideal $Cu_{0.5}Li_{0.5}InSe_2$ (Fig. 4) compared to the corresponding ideal case (Fig. 7(c)). The sharp peak comes due to the contribution of Se-p orbitals. But in case of ideal $Cu_{0.5}Li_{0.5}InSe_2$, DOS is high in Cu d orbitals. There are effects on conduction band also. This shows that structural distortion not only decreases the band gap but it has significant effect on overall electronic properties as well. Similar results are also found for $CuInSe_2$ and $CuIn_2Se_4$ systems. For these two compounds we can find significant effect of structural distortion on band gap. The effect of distortion on valence and conduction bands show that structural distortion is also responsible for significant change in optical properties of such semiconductors.

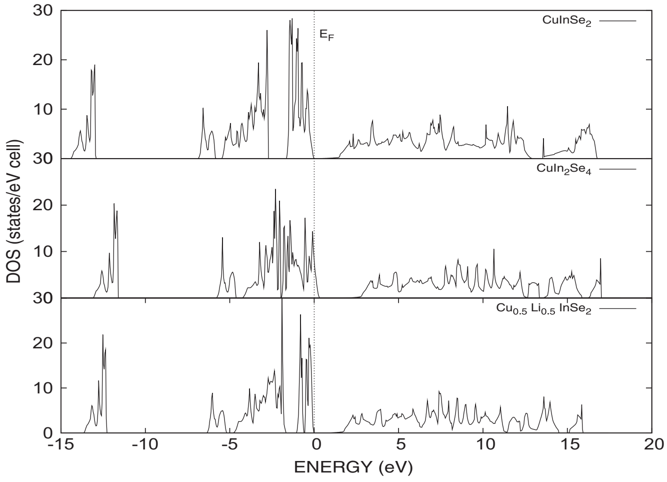

Fig. 7. TDOS for ideal and with hybridization of (a) $CuInSe_2$, (b) $CuIn_2Se_4$ and (c) $Cu_{0.5}Li_{0.5}InSe_2$.

3.5. Bond nature

In case of $CuInSe_2$, bond lengths of Cu–Se and In–Se agree well with experimental bond lengths mentioned in [24]. In $CuInSe_2$ the covalent bonding character of the Cu–Se bonding is dominant. When covalent character dominates, Se p–Cu d hybridization plays a major role. This causes a greater narrowing down of the band gap in the case of $CuInSe_2$ compared to the other two compounds. This is because there are 50% less Cu–Se bonds in defect and Li-substituted $CuInSe_2$. The Li–Se bonding possesses an ionic character because of the large electronegativity difference between Li and Se atoms. This ionic character of bonding increases the band gap in $Cu_{0.5}Li_{0.5}InSe_2$.

4. Conclusion

Calculations and study of $CuInSe_2$, $CuIn_2Se_4$ and $Cu_{0.5}Li_{0.5}InSe_2$ suggest that these compounds are direct band gap semiconductors with band gaps of 0.79 eV, 1.50 eV and 1.08 eV, respectively. Our study further shows that electronic properties of these semiconductors significantly depend on the type of hybridization and structural distortion. The calculation is carried out using DFT based TB-LMTO method. We use LDA for our exchange corelation functional. Taking into account the underestimation of band gap by LDA, our result of band gap and structural properties agree with experimental values. Detailed studies of the TDOS and PDOS show that p–d hybridization between Cu d and Se p orbitals reduces the band gap compared to what one would expect if Cu d orbitals did not have an influence on the band structure. The reduction is 59.57%, 23.61% and 48.82%, respectively, for $CuInSe_2$, $CuIn_2Se_4$ and $Cu_{0.5}Li_{0.5}InSe_2$. Li-substitution in $CuInSe_2$ shifts Se p orbitals in the conduction band towards the Fermi level which eventually reduces the band gap. Decreament of the band gap due to structural distortion is 16.85%, 9.10% and 0.92% in case of $CuInSe_2$, $CuIn_2Se_4$ and $Cu_{0.5}Li_{0.5}InSe_2$, respectively.

Acknowledgements

This work was supported by Department of Science and Technology, India, under the grant no. SR/S2/CMP-26/2007. We would like to thank Prof. O.K. Andersen, Max Planck Institute, Stuttgart, Germany, for kind permission to use the TB-LMTO code developed by his group.

References

[1] J.L. Shay, I.H. Wernick, Ternary Chalcopyrite Semiconductors: Growth, Electronic Properties and Applications, Pergamon Press, New York, 1975.
[2] J.E. Bernard, A. Zunger, Phys. Rev. B 37 (1988) 6835–6856.
[3] L.I. Koroleva, D.M. Zashchirinskii, T.M. Khapaeva, S.F. Marenkin, I.V. Fedorchenko, R. Szymczak, B. Krzumnska, V. Dobrovol'skii, L. Kilanskii, Phys. Solid State 51 (2009) 303.
[4] T.Y. Park, J.Y.Oh Lim, S.K. Park, K.H. Song, H.J. Kim, W.T. Choe, S.H. Kim, C.D. Yoon, C. Sun, J. Appl. Phys. 84 (1998) 1567.
[5] L.L. Kazmerski, Nuovo Cimento D 2 (1983) 2013.

[6] O. Madelung, in: O. Madelung (Ed.), Numerical Data and Functional Relationship in Science and Technology, Landolt-Börnstein, New Series, vol. 17h, Springer, Berlin, 1985.
[7] M. Suzuki, T. Uenoyama, T. Wada, T. Hanada, Y. Nakamura, Jpn. J. Appl. Phys. 36 (1997) L1139–L1141.
[8] S. Mitaray, G. Kühn, B. Schumann, A. Tempel, Thin Solid Films 135 (1986) 251–256.
[9] S. Weise, E. Nowaka, A. Lenz, B. Schumann, V. Krämer, J. Cryst. Growth 166 (1996) 718–721.
[10] D. Azulaya, O. Millo, I. Balberga, H.W. Schock, I. Visoly-Fisher, D. Cahen, Sol. Energy Mater. Sol. Cells 91 (2007) 85–90.
[11] S.M. Wasim, Sol. Cells 16 (1986) 289–316.
[12] M.I. Alonso, K. Wakita, J. Pascual, M. Garriga, N. Yamamoto, Phys. Rev. B 63 (2001) 075203.
[13] T.M. Hsu, J. Appl. Phys. 69 (1991) 3772–3774.
[14] J.E. Jaffe, A. Zunger, Phys. Rev. B 27 (1983) 5176–5179.
[15] J.E. Jaffe, A. Zunger, Phys. Rev. B 29 (1984) 1882.
[16] S. Mishra, B. Ganguli, Solid State Commun. 151 (2011) 523–528.
[17] S. Mishra, B. Ganguli, J. Solid State Chem. 184 (2011) 1614–1621.
[18] X.S. Jiang, S. Mi, P.J. Sun, Y. Lu, J.Q. Liang, Chin. Phys. Lett. 26 (2009) 077102.
[19] W. Kohn, L.J. Sham, Phys. Rev. A 140 (1965) 1133.
[20] O.K. Andersen, Phys. Rev. B 12 (1975) 3060.
[21] O. Jepsen, O.K. Andersen, Solid Sate Commun. 9 (1971) 1763.
[22] P. Hohenberg, W. Kohn, Phys. Rev. B 136 (1964) 864.
[23] U. Barth, L. Hedin, J. Phys. C: Solid State Phys. 5 (1972) 1629.
[24] J. Parkes, R.D. Tomlinson, M.J. Hampshire, J. Appl. Cryst. 6 (1973) 414–416.
[25] E. Gusev, Defects in High-k Gates Dielectric Stacks, NATO Science Series II, Mathematics, Physics and Chemistry, Springer, New York, 2006.
[26] A. Miller, A. Mackinnon, D. Weaire, in: H. Ehrenreich, F. Seitz, D. Turubull (Eds.), Solid State Physics, vol. 36, Academic, New York, 1981.